ELSEVIER

Biophysical Chemistry 124 (2006) 214–221

Biophysical Chemistry

http://www.elsevier.com/locate/biophyschem

# The stability and characteristics of a DNA Holliday junction switch

A.R. Mount [a,*], C.P. Mountford [b], S.A.G. Evans [a], T.-J. Su [c], A.H. Buck [c], P. Dickinson [c], C.J. Campbell [c], L.M. Keane [c], J.G. Terry [d], J.S. Beattie [c], A.J. Walton [d], P. Ghazal [c], J. Crain [b]

[a] *School of Chemistry, The University of Edinburgh, Mayfield Road, Edinburgh EH9 3JJ, UK*
[b] *School of Physics, The University of Edinburgh, Mayfield Road, Edinburgh EH9 3JZ, UK*
[c] *The Scottish Centre for Genomic Technology and Informatics, The University of Edinburgh, The Chancellor's Building, 49 Little France Crescent, Edinburgh, EH16 4SB Scotland, UK*
[d] *Institute of Integrated Micro and Nano Systems, Scottish Microelectronics Centre, School of Engineering and Electronics, University of Edinburgh, Edinburgh, EH9 3JF, UK*

Received 17 January 2006; accepted 25 March 2006
Available online 6 April 2006

**Abstract**

A Holliday junction (HJ) consists of four DNA double helices, with a branch point discontinuity at the intersection of the component strands. At low ionic strength, the HJ adopts an open conformation, with four widely spaced arms, primarily due to strong electrostatic repulsion between the phosphate groups on the backbones. At high ionic strength, screening of this repulsion induces a switch to a more compact (closed) junction conformation. Fluorescent labelling with dyes placed on the HJ arms allows this conformational switch to be detected optically using fluorescence resonance energy transfer (FRET), producing a sensitive fluorescent output of the switch state. This paper presents a systematic and quantitative survey of the switch characteristics of such a labelled HJ. A short HJ (arm length 8 bp) is shown to be prone to dissociation at low switching ion concentration, whereas an HJ of arm length 12 bp is shown to be stable over all switching ion concentrations studied. The switching characteristics of this HJ have been systematically and quantitatively studied for a variety of switching ions, by measuring the required ion concentration, the sharpness of the switching transition and the fluorescent output intensity of the open and closed states. This stable HJ is shown to have favourable switch characteristics for a number of inorganic switching ions, making it a promising candidate for use in nanoscale biomolecular switch devices.


*Keywords:* Holliday junction; FRET; Biomolecular switch; DNA; Stability; Ion control

## 1. Introduction

The structural properties that make DNA capable of conferring genetic information also enable it to behave as a scaffolding unit for DNA nanotechnology [1] and also as a processing unit for DNA-based computation [2,3]. In recent years, much research has focused on the design and implementation of DNA-based functional building blocks for the production of nanodevices [4]. Holliday junctions (HJ) and related structures [5] are likely to be particularly versatile as they can potentially act as both structural scaffolding units in nanodevices and as active elements capable of reporting on local environmental changes via ion-induced conformational transitions. The DNA Holliday structure is a junction of four double helices, first proposed in 1964 [6]. The unique topological element of the junction is a branch point at the intersection of the component strands. The junction exists in either open or closed forms, determined primarily by the strong electrostatic repulsion between the backbone phosphate groups. In low ionic strength solutions, this repulsive coulombic interaction favors an extended structure determined by maximum charge separation, an open branch point region and approximate fourfold symmetry. The open form has also been identified in certain crystal structures of the junction in complexes with recombination and repair proteins [7].

In high ionic strength solutions, screening of the repulsion between phosphate groups on the DNA backbone induces a conformational transition to a more compact, folded junction; the branch point collapses to enable pairs of double helical arms

* Corresponding author. Tel.: +44 131 650 4747; fax: +44 131 650 4743.
*E-mail address:* A.Mount@ed.ac.uk (A.R. Mount).

0301-4622/$ - see front matter © 2006 Elsevier B.V. All rights reserved.
doi:10.1016/j.bpc.2006.03.020

to align coaxially and cross in one of two so-called stacked-X (closed) conformations [8–10]. It is believed that the stacked-X junction may undergo rapid isomerisation transitions between these two forms as suggested by recent single molecule measurements [11]. Schematic open and closed structures are shown in Fig. 1.

Several ions have now been shown to be effective promoters of junction folding. The most extensively studied are the divalent metals $Mg^{2+}$ and $Ca^{2+}$, but switching at lower concentrations is also observed for the trivalent $[Co(NH_3)_6]^{3+}$ cation [10,12,13]. Structural studies of the stacked configuration are relatively rare though X-ray, NMR [14] and simulation [15] techniques have revealed likely binding site locations [16]. Most of the interest in the structure and properties of branched DNA intermediates arises from their importance in genetic recombination processes [6], recognition and processing by proteins [17], viral integration [18] and DNA repair [19].

Despite being structurally well characterized [20–23] there have been no systematic, quantitative explorations of the switching characteristics of an HJ. In this paper we carry out such an exploration, with a view to assessing suitability of HJs as components in nanoscale switch devices. As there is doubt over the stability of HJ structures produced from relatively short strands [24], HJ stability at two different strand lengths was first assessed using gel electrophoresis, prior to determining the switching characteristics of the stable HJ. The issues relevant in this context include switching ion concentration, sharpness of the ion-induced switching transition and fluorescence output of switch state. The practical issue of how ionic strength and pH can be controlled without inducing appreciable switching is important for biomolecular interactions and this is also investigated.

## 2. Experimental

### 2.1. Chemicals

All solutions were prepared using deionised water from a Whatman RO 15 water purification system (resistivity ≥ 18 MΩ cm) using a 0.22 μm filter, and all compounds were used as received without further purification. Hydrochloric acid (purity 99.999%), Tris-(hydroxymethyl)aminomethane (Tris, Ultrapure), Nitric acid (purity 99.99%), and spermidine trichloride (purity 99%) were obtained from Aldrich. Lithium chloride, sodium chloride (AnalaR) and sulfuric acid (AnalaR) were obtained from BDH, potassium chloride and calcium chloride (Laboratory Reagent Grade) were purchased from Fisons Scientific equipment. Magnesium chloride hexahydrate (purity > 99.5%) and tetramethylammonium chloride (purity > 98%) were obtained from Fluka Chemika.

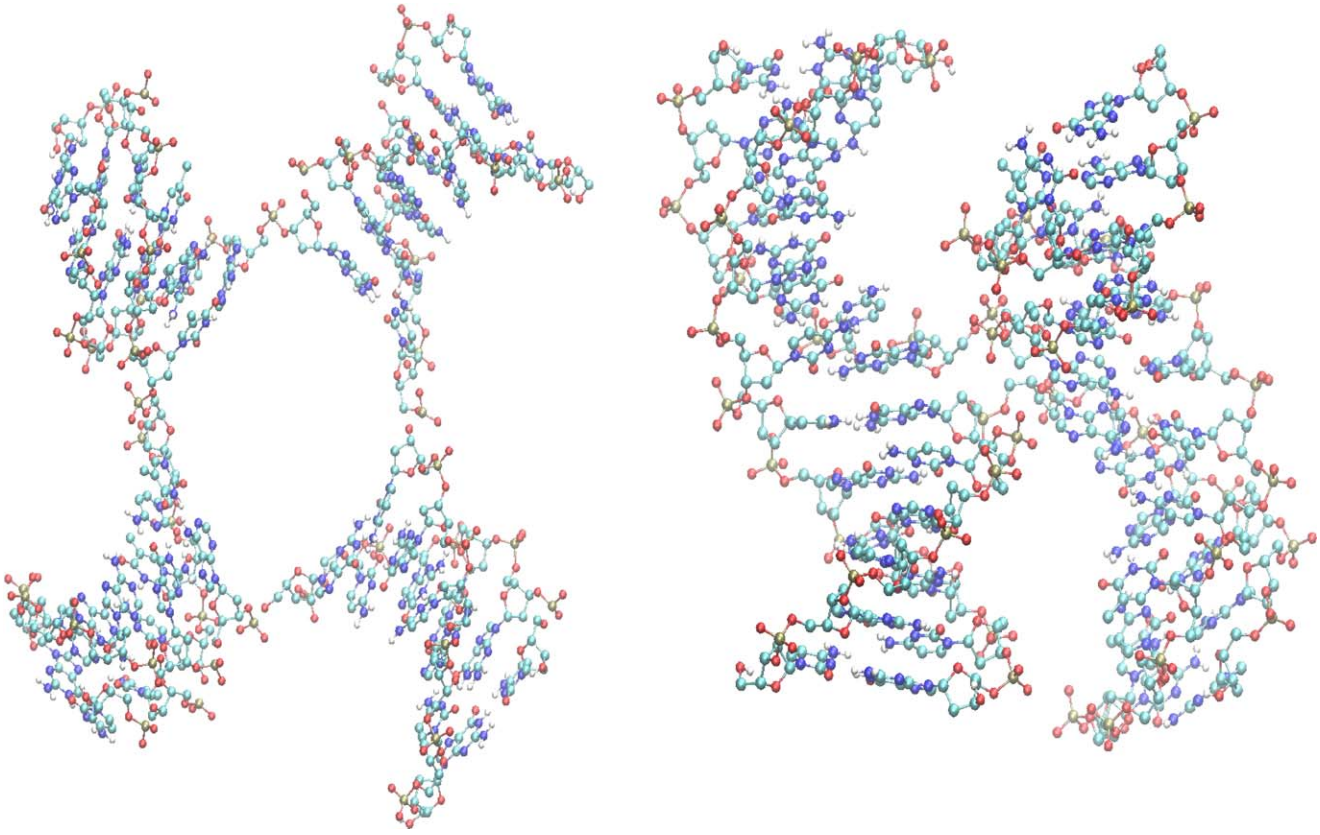

Fig. 1. Schematic of a Holliday junction. In the absence of switching cations the junction is in the open configuration with a maximally extended square-planar structure (left). At high ionic strength, electrostatic repulsion of the phosphate groups on the backbones is reduced, resulting in helix–helix stacking and the closed conformation (right).

### 2.2. Construction of four-way junctions

A short-armed DNA-junction (SHJ) was prepared from a mixture of the following four pure oligonucleotides (Eurogentec):

**F**TGCAATCCTGAGCACA (5 μM, **1**),
TGTGCTCACCGAATCGGA (10 μM, **2**),
TCCGATTCGGACTATGCA (10 μM, **3**)
**R**TGCATAGTGATTGCA (10 μM, **4**).

**F** is the donor Carboxyfluorescein (known commercially as FAM™) on oligonucleotide **1** and **R** is the acceptor Carboxytetramethylrhodamine (known as TAMRA™) on oligonucleotide **4**. A corresponding longer armed junction (LHJ), which has 4-bp extensions to each arm due to the addition of complementary bases (shown in italics) to the ends of the SHJ arms, was prepared from (Eurogentec):

*GGCA***F**TGCAATCCTGAGCACA*TAGA* (5 μM, **1**),
*TCTA*TGTGCTCACCGAATCGGA*CCAG* (10 μM, **2**),
*CTGG*TCCGATTCGGACTATGCA*GCAA* (10 μM, **3**),
*TTGC***R**TGCATAGTGATTGCA*TGCC* (10 μM, **4**)

In this case, internal dyes were used to maintain dye position relative to the branch point. Each was assembled in a solution of 20 mM Tris/Tris$H^+Cl^-$ (pH 7.5) buffer solution containing NaCl (50 mM) and $MgCl_2$ (5 mM), by heating to 80 °C for 30 min and then allowing the solution to cool slowly in a water bath to room temperature, which favours the thermodynamically most stable product. A ratio of 1 : 2 : 2 : 2 of oligonucleotide **1**:**2**:**3**:**4** was chosen to ensure full incorporation of donor strand into the fully assembled 4-way junctions. Typically, the final step in the sample preparation was to buffer exchange twice (Microspin G25 ion exchange columns (Amersham Biosciences)), to remove the $Mg^{2+}$ ions and produce HJ solutions (concentration 1 μM after dilution) in 20 mM Tris/Tris$H^+Cl^-$ buffer (pH 7.5) as required for ion titration studies. 100 μM tetrasodium ethylenediamine(tetraacetate) ($Na_4EDTA$) was then added to the solution to titrate any residual $Mg^{2+}$ ions and produce HJ exclusively in the open form, as confirmed by characteristic and time independent steady-state fluorescence measurements (for titration studies, 100 μM was then subtracted from the concentration, *c*, of the inorganic ions which would be expected to complex strongly with EDTA. This was confirmed by the invariance of the steady-state emission when adding an initial 100 μM of these inorganic ions).

### 2.3. HJ stability

#### 2.3.1. Gel electrophoresis

For gel electrophoresis assays, all oligonucleotide preparations were made at 10 μM in equimolar concentrations as described above (except for the assembled HJ which was made at the standard 5 μM : 10 μM : 10 μM : 10 μM ratio, see Section 2.2) and buffer exchanged twice into 45 mM Tris/Tris$H^+$Borate (pH 8.3). $MgCl_2$ was added to give a final concentration of 0.25 mM and 4 μl (approximately 250 ng) of each sample was loaded as a band onto a 10% polyacrylamide gel in 45 mM Tris/Tris$H^+$Borate (pH 8.3), 0.25 mM $MgCl_2$ electrophoresis buffer.

Samples were loaded in the following order: Oligonucleotides **1**, **2**, **3** and **4** individually, in pairwise combinations **2**+**3** and **3**+**4**, as a 3-way structure **2**+**3**+**4** and as the assembled 4-way HJ structure, **1**+**2**+**3**+**4**. Additionally, TGCAATCCTGAGCACATTTTT**F**GTGCTCACCGAATCGGATTTT**R**TCCGATTCGGACTATGCA (**5**), was also deposited as a control oligonucleotide band. This is a 60-mer, containing internal Carboxyfluorescein (**F**) and Carboxytetramethylrhodamine (**R**) labelled dT (where dT is deoxythymidine), which is expected to be of comparable size to the fully assembled SHJ. The gel was run for 4.5 h at 4 °C at 6.25 V/cm and then fixed in 45 mM Tris/Tris$H^+$Borate containing 7% (v/v) acetic acid, 10% (v/v) isopropanol for 15 min, stained in 45 mM Tris/Tris$H^+$Borate containing 0.02% (w/v) stains-all dye (Aldrich), 20% (v/v) formamide, 20% (v/v) isopropanol for 30 min in the dark and destained in Tris/Tris$H^+$Borate containing 10% (v/v) isopropanol in the light for 90 min. The gel was then scanned on a flatbed scanner to capture 8-bit grey scale images.

#### 2.3.2. gelFRET assays

gelFRET assays were performed as described elsewhere [25]. HJ solutions (1 μM) in 45 mM Tris/Borate pH 8.3 buffer were prepared in the presence of either 0 or 5.0 mM $MgCl_2$ and were loaded onto gels (10% acrylamide, 45 mM Tris/Borate pH 8.3, and 0 or 5.0 mM $MgCl_2$ as appropriate). Gels were run at 4 °C with an electric field of 7 V/cm for 2 h, and then scanned with a Typhoon 9400 scanner (Amersham Biosciences): laser light at 488 nm was used to excite the donor. The emitted light was passed through either a 526-nm short-pass filter (for donor emission) or a 580-nm band-pass filter (for acceptor emission). Using ImageQuant software (Molecular Dynamics), the intensity of the signal obtained at 526 nm (represented by the intensity of the colour green) was overlaid with the intensity of the signal obtained at 580 nm (represented as the intensity of the colour red) to visualize the relative difference in FRET for each gel band.

### 2.4. Fluorescence spectroscopy

As in several previous HJ structural studies [20–23], the switching of the assembled 4-way junction was detected optically using fluorescence resonance energy transfer (FRET) between the donor (**F**) and acceptor (**R**) fluorophores. Steady-state fluorescence emission spectra were recorded in a Starna 26.5-F Far UV quartz fluorescent cell (10 mm path length) using a Jobin Yvon Spex Fluoromax spectrofluorimeter (Instruments S.A.) with a fixed excitation wavelength of 476.5 nm. This wavelength was chosen to maximize donor excitation while minimizing direct excitation of the acceptor molecule. This was confirmed by control experiments, which showed 1 μM short-armed oligonucleotide **4** to have peak acceptor emission of less than 5% of the peak donor emission of 1 μM oligonucleotide **1** at this wavelength.

### 2.5. Titration protocol

Titrations involved adding aliquots of a concentrated cation solution in 20 mM Tris/Tris$H^+Cl^-$ buffer to a 50 μl solution of 1.0 μM HJ, prepared as in Section 2.2. The solution was then thoroughly mixed and left to equilibrate for at least 2 min (which experiments showed was sufficient to ensure equilibration) before recording the steady-state emission spectra. The intensity of each spectrum was adjusted for the increase in volume on titration to allow for the effects of dilution. For the $TrisH^+$ titration experiment, aliquots of a concentrated (2.0 M in Tris) solution of Tris/Tris$H^+Cl^-$ buffer (pH 7.5) were added to achieve the desired cation concentration change, while maintaining a constant pH. Non-linear least squares curve fitting of data to Eqs. (7) and (8) and calculation of errors and reduced $\chi^2$ values was carried out using Origin (MicroCal).

## 3. Results and discussion

### 3.1. Switch formation and integrity

Although other DNA machines have been demonstrated which rely on assembly/disassembly processes [26], for the purpose of this work we have only considered a workable switch to be one which changes conformation without disassembly at defined low and high switching ion concentrations. Gel electrophoresis of the SHJ in 0.25 mM $MgCl_2$ (Fig. 2a), a relatively low $Mg^{2+}$ ion concentration consistent with the HJ being predominantly in the open configuration (Section 3.3; Table 1), shows the predominant SHJ band (lane 8) to migrate much more slowly than the individual or dimerised oligonucleotides and at a similar rate to the control oligonucleotide (lane 9). This band can therefore be assigned to the assembled 4-way SHJ.

However, there are also faster migrating bands of significant intensity in lane 8, which by comparison with lanes 1–7 can be attributed to the single oligonucleotides and a dimer assembly product of oligonucleotides **2** and **3**. These bands are much more prominent than those observed on similar gels at 5 mM $MgCl_2$, which indicates that significant SHJ disassembly is occurring at low $Mg^{2+}$ concentration. This is consistent with previous studies, which showed that other HJs of slightly shorter DNA length than SHJ dissociate under comparable switching ion concentrations [24]. It is interesting that oligonucleotides **2** and **3** are seen to be most likely to form a dimer complex. This can be attributed to their relatively long complementary 10 bp overlap, compared to 8 bp for oligonucleotides **3** and **4**. This suggests that an increase in oligonucleotide lengths could lead to a higher degree of association, thereby stabilising the assembled HJ and producing less dissociation for LHJ compared to SHJ. Fig. 2b shows gelFRET experiments carried out on both SHJ and LHJ in the presence and absence of $Mg^{2+}$ switching ion. In the absence of $Mg^{2+}$ no band due to SHJ can be seen, whereas LHJ retains a single band. This supports the complete dissociation of SHJ under these conditions and also indicates that in the absence of switching ions, the extra base pairing in LHJ is sufficient to overcome the tendency of SHJ to dissociate. However, both

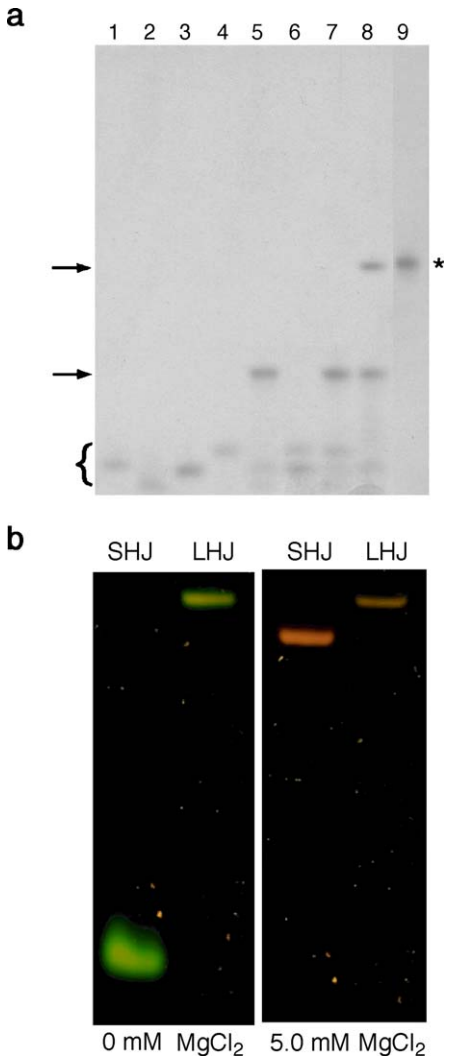


Fig. 2. (a) Electrophoresis to demonstrate the stability of the 4-way SHJ structure at low switching ion concentration (0.25 mM $Mg^{2+}$). The gel shows bands correspond to each individual oligonucleotide 1 to 4 (lanes 1–4), mixtures of: oligonucleotides 2+3 (lane 5), oligonucleotides 3+4 (lane 6), oligonucleotides 2+3+4 (lane 7), the 4-way SHJ assembled from oligonucleotides 1+2+3+4 (lane 8) and oligonucleotide **5** (lane 9), with migration from top to bottom. Positions of monomer oligonucleotides are indicated by a bracket. Dimers formed between oligonucleotides 2+3 are indicated by the lower arrow. The upper arrow indicates the presence of a band representing the intact 4-way SHJ structure in lane 8, migrating at a position similar to that of the 60-mer oligonucleotide control **5** of similar size (indicated by *) in lane 9. (b) gelFRET data to assess the stability and switching characteristics of 4-way SHJ and LHJ in the total absence (open conformation) and presence (closed conformation) of $Mg^{2+}$ switching ion. Without $Mg^{2+}$, SHJ is seen to give a fast migrating band due to SHJ dissociation. In contrast, LHJ shows a band consistent with retention of the 4-way HJ structure under both conditions. Both LHJ and SHJ show minimal FRET (overall green colour) in the absence of $Mg^{2+}$ but significant FRET (overall red) in the presence of $Mg^{2+}$, consistent with $Mg^{2+}$ ion-induced HJ switching. (For interpretation of the references to colour in this figure legend, the reader is referred to the web version of this article.)

SHJ and LHJ show single bands in the presence of $Mg^{2+}$, with (as expected based on size) LHJ migrating slightly more slowly than the SHJ. Furthermore, the FRET data confirms that both SHJ and LHJ show a change from low FRET (overall bright green, relatively high intensity) in the absence of $Mg^{2+}$ to high relative FRET (overall bright red, relatively high intensity) at

5 mM $Mg^{2+}$, consistent with both adopting the closed conformation at 5 mM $Mg^{2+}$. In the case of LHJ, this indicates a functional switch which maintains its integrity even in the absence of $Mg^{2+}$, whereas SHJ is a switch whose assembled stability *and* switching is $Mg^{2+}$-dependent.

### 3.2. LHJ switching characteristics

Fig. 3a and b shows typical LHJ fluorescence emission spectra obtained as a function of the concentration of $Mg^{2+}$ and $Na^{+}$ switching ions, respectively.

At relatively low switching ion concentration, *c*, it is clear in both cases that an emission peak is seen at around 517 nm. This is characteristic of **F** donor emission, which decreases in intensity with increasing *c* at the expense of a growing peak at around 584 nm, characteristic of **R** acceptor emission and therefore indicative of FRET. Given the strong inverse sixth power dependence of FRET efficiency on the donor–acceptor separation distance, this is consistent with previous observations [20,22] of a growing proportion of folded (closed) HJs

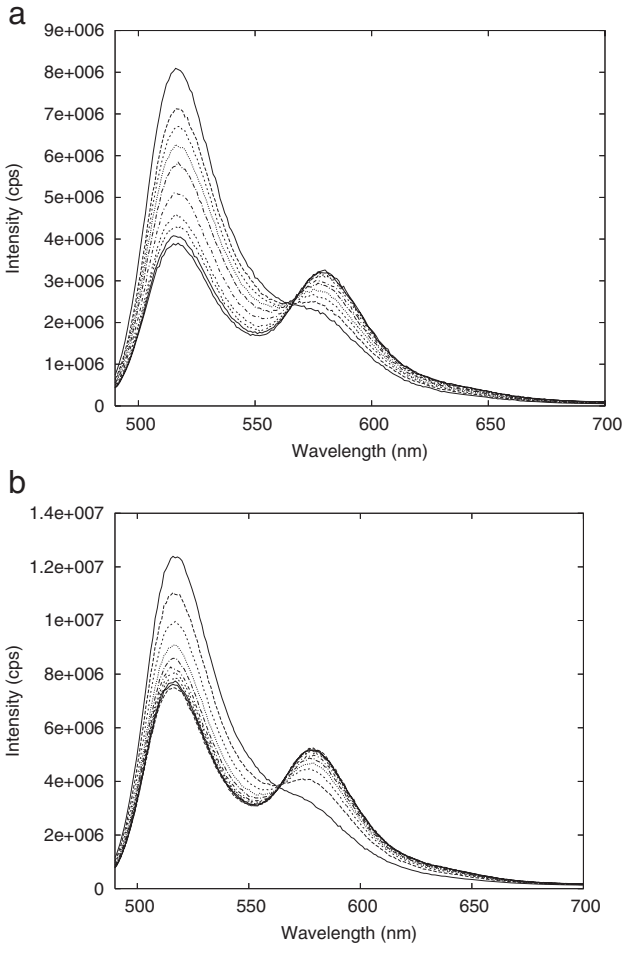


Fig. 3. Fluorescence emission spectra for a solution of 1 μM LHJ in 20 mM pH 7.5 Tris/$TrisH^{+}Cl^{-}$ buffer (Tris buffer), titrated with increasing concentration of (a) $Mg^{2+}$ between 100 μM and 9.8 mM and (b) $Na^{+}$ between 55 and 410 mM. In each case, the conversion from the open (maximum emission at 517 nm) to the closed configuration (which shows a FRET peak with a maximum emission at 584 nm) can clearly be seen, along with the isosbestic point at 564–565 nm.

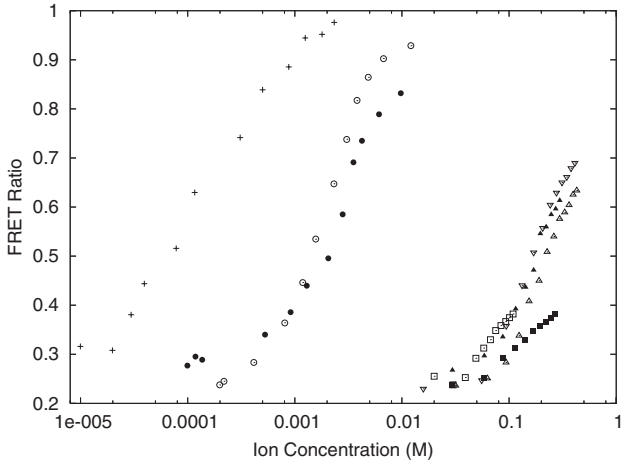


Fig. 4. Plots of FRET ratio versus ion concentration data obtained when titrating the ions (■) $TMA^{+}$, (□) $TrisH^{+}$, (▽) $Na^{+}$, (△) $Li^{+}$, (▲) $K^{+}$, (●) $Mg^{2+}$, (○) $Ca^{2+}$and (+) the spermidine ion ($\{H_3N(CH_2)_3NH_2(CH_2)_4NH_3\}^{3+}(Sp^{3+})$) into a solution of 1 μM open HJ in Tris buffer. Ion concentrations have been adjusted for the presence of EDTA.

which show FRET due to the effects of cation-induced folding, at the expense of open HJs which show no FRET.

The results of further measurements are summarized in Fig. 4 for both monovalent, and multivalent ions where we present the increase of FRET signal as the ratio of the peak acceptor intensity ($I_A$) to the donor intensity ($I_D$). In general, consistent with previous observations [13], we find the basic trend that the cation concentration threshold (the minimum concentration required to actuate the switch) decreases markedly with increasing valency. This is fully consistent with the overall notion that the electrostatic repulsion between fixed phosphate backbone charges must be sufficiently screened by switching ions to enable folding. It is thus clear that much larger ion concentrations are required for monovalent ions to induce switching and switching due to monovalent ions can be ignored when multivalent ions are present. The effect of buffer cation concentration on HJ conformation has not been considered in previous studies; this work confirms the applicability of $TrisH^{+}$ as an inert buffer ion, maintaining constant pH and high ionic strength, while not inducing significant folding at the tens of millimolar ion concentrations required for solution buffering.

### 3.3. Assessment of LHJ switching

#### 3.3.1. Quantitative analysis of HJ switching with inorganic ions

An important feature of Fig. 3 (and all other ion titration data) is the significant acceptor emission intensity relative to the donor emission intensity seen for the closed form. This is consistent with our branch point sequence design (which is based on the well-studied "J1" structure [27,28], which is a sequence designed to cause the vast majority of the closed LHJ to adopt the FRET signal conformer, maximising acceptor emission output [23]). Also significant is the presence of an isosbestic point for each of the ions at 564–565 nm, where the overall intensity, $I_{iso}$, of the fluorescence emission is

independent of $Mg^{2+}$ and $Na^{+}$ ion concentration, respectively. This is strong evidence for fluorescence emission arising from only two states of the assembled HJ molecule (one FRET inactive, open and one FRET active, closed), as the fluorescence emission intensity obeys Eqs. (1) and (2) in this range of concentrations

$$I(\lambda) = I_{\text{open}}(\lambda)x_{\text{open}} + I_{\text{closed}}(\lambda)x_{\text{closed}} \quad (1)$$

with

$$x_{\text{open}} = 1 - x_{\text{closed}} \quad (2)$$

where $I_{\text{open}}$ and $I_{\text{closed}}$, the emission intensities of the HJ solution when entirely in the open and closed forms, respectively, are equal at 564–565 nm, and $x_{\text{open}}$, $x_{\text{closed}}$ are the mole fractions of the open and closed forms. This is consistent with the previous postulate of two-state switching for a similar HJ system [22]. $I_{\text{open}}$ and $I_{\text{closed}}$ are related to the fundamental emission characteristics of the open and closed HJs, respectively, and must be independent of ion concentration ($c$). These can be obtained at all wavelengths from experimental steady-state emission spectra at low ($c \to 0$) and high ($c \to \infty$) switching ion concentrations respectively, these conditions being denoted by superscript 0 and ∞. At any $c$, independent experimental values of $x_{\text{open}}$ and $x_{\text{closed}}$ can most accurately be obtained at the peak donor and acceptor wavelengths, $I_D$ and $I_A$, respectively, by combining Eqs. (1) and (2) to give:

$$x_{\text{open}} = \frac{I_D - I_D^{\infty}}{I_D^{0} - I_D^{\infty}} \quad (3)$$

and

$$x_{\text{closed}} = \frac{I_A - I_A^{0}}{I_A^{\infty} - I_A^{0}} \quad (4)$$

Fig. 5 shows typical plots of calculated values of $x_{\text{open}}$ and $x_{\text{closed}}$ as functions of $c$ determined from equivalent data to Fig. 3 for both $Ca^{2+}$ and $Li^{+}$.

Notwithstanding the very different switching ion concentrations, it is clear that for each of these plots (and for all the inorganic ions studied) Eq. (2) applies at all $c$. This further supports the general applicability of the two-state model, Eq. (1) and the invariance of $I_{\text{open}}$ and $I_{\text{closed}}$ with $c$ at these wavelengths.

*3.3.1.1. LHJ folding thermodynamics.* For thermodynamic quantitation of two-state HJ switching through ion binding, the simplest approach is to assume the establishment of the dynamic equilibrium

$$HJ_{\text{closed}} \leftrightarrow HJ_{\text{open}} + nM^{z+} \quad (5)$$

where $K$ is the dissociation constant for the switching equilibrium and $M^{z+}$ is the switching ion. In this case, neglecting activity coefficients (under these conditions of approximately constant ionic strength):

$$K = \frac{x_{\text{open}}}{x_{\text{closed}}} c^n = c_{1/2}^n \quad (6)$$

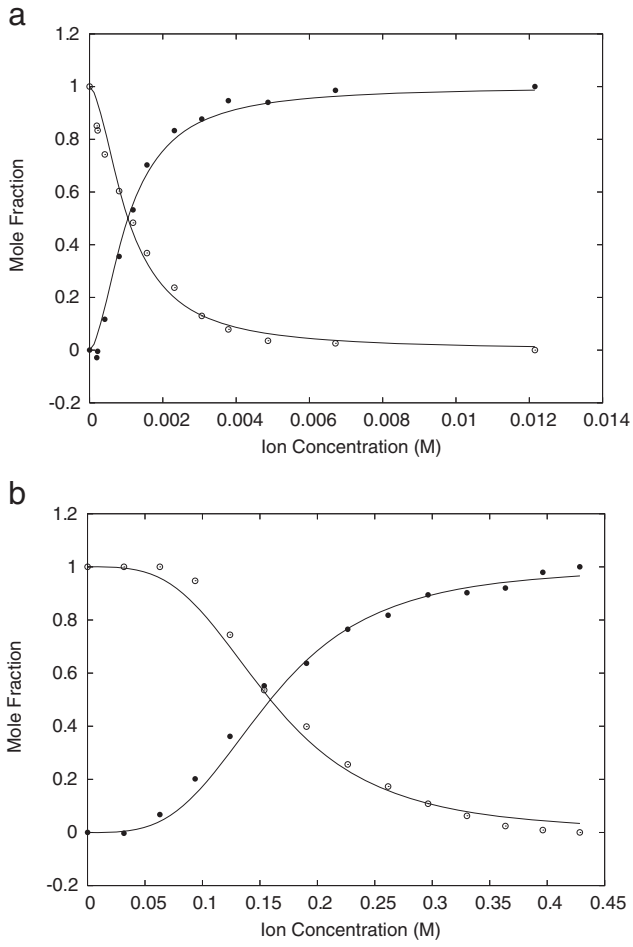


Fig. 5. Plot of the fraction of open (○) and closed (●) HJ versus (a) $Ca^{2+}$ and (b) $Li^{+}$ concentration in a solution of 1 μM HJ in Tris buffer. The solid lines show the theoretical fits to Eqs. (7) and (8).

where $c_{1/2}$ is the ion concentration at which $x_{\text{open}} = x_{\text{closed}} = 1/2$. Combining Eqs. (2) and (6) then gives

$$x_{\text{open}} = \frac{c_{1/2}^n}{c_{1/2}^n + c^n} \quad (7)$$

and

$$x_{\text{closed}} = \frac{c^n}{c_{1/2}^n + c^n} \quad (8)$$

Fig. 5 shows typical combined theoretical fits, with simultaneous non-linear least squares analysis, to Eqs. (7) and (8) for the experimental open and closed LHJ data. The close correspondence of this simple two-state model with experiment is highly satisfactory and confirms the action of a switch. From each of these plots a value of $c_{1/2}$ and of $n$ is obtained. These are independent parameters; $c_{1/2}$ determines the location of the switching transition on the concentration axis and is inversely related to the ion binding strength; $n$ determines the sharpness of the transition and is analogous to the Hill coefficient [29]. High values of $n$ therefore equate to sharp switching, where switching between the two forms occurs over a relatively narrow concentration range. The sharpness of this transition between

Table 1
Quantitative analysis parameters for LHJ switching at 1 μM unless otherwise stated

| $M^{z+}$ | Buffer | $c_{1/2}$ (mM) | $n$ | $\chi^2$ |
|---|---|---|---|---|
| $Li^+$ | Tris/HCl | 159±3 | 3.4±0.2 | 0.001 |
| $Na^+$ | Tris/HCl | 126±3 | 3.1±0.2 | 0.002 |
| $K^+$ | Tris/HCl | 120±2 | 3.3±0.2 | 0.001 |
| $Ca^{2+}$ | Tris/HCl | 1.1±0.1 | 1.8±0.1 | 0.002 |
| $Mg^{2+}$ | Tris/HCl | 1.2±0.1 | 1.3±0.1 | 0.004 |
| $Mg^{2+}$, 0.2 μM HJ | Tris/HCl | 1.6±0.1 | 1.6±0.1 | 0.005 |

$\chi^2$ gives the reduced chi-squared values for the 2-parameter non-linear least squares fits to the data.

the "on" and "off" states is a key characteristic that defines how close the system is to a theoretically ideal switch.

Table 1 shows typical experimental values of $c_{1/2}$ and $n$ calculated for a variety of switching ions.

The low values of reduced $\chi^2$ demonstrate that this relatively simple analysis produces good fits to the data for all ions. The values of $n$ are all greater than 1, which is physically realistic, as at least one ion is required to induce switching. Within the ion groups ($Li^+$, $Na^+$ and $K^+$) and ($Mg^{2+}$ and $Ca^{2+}$), which have the same cation charge, $z$, the values of $c_{1/2}$ and $n$ are similar. As both the solvated and unsolvated ion sizes vary greatly for these ions, this indicates that neither hydrated or dehydrated ion size determines LHJ folding characteristics. However, there is a strong dependency of $c_{1/2}$ on $z$, as increasing $z$ from +1 to +2 decreases $c_{1/2}$ by approximately 100-fold. This is a much larger effect than the $z^{-2}$ dependency expected for interactions controlled simply by ionic strength (such as colloidal coagulation), which is evidence for more specific cation–backbone phosphate interactions. The value of $n$ also changes markedly, being close to 3 for $Li^+$, $Na^+$ and $K^+$ and between 1 and 2 for $Mg^{2+}$ and $Ca^{2+}$. Under conditions of positive cooperativity, where multiple ions bind successively with increasingly tight binding (larger binding affinities) [29], $n$ is equal to the minimum number of ions which are required to associate to induce folding. Even in other more complicated cases, values of $n$ greater than 1 indicate multiple ion binding [29]. This value could suggest that divalent ions are better able to electrostatically interact with multiple backbone phosphate groups and hence fewer are required to induce folding than for monovalent ions.

Finally, values of $c_{1/2}$ and $n$ obtained for 1 μM HJ and 0.2 μM HJ (Table 1) can be seen to be similar. This similarity is further evidence for the retention of the fully assembled LHJ at both of these concentrations, the applicability of Eq. (5) and the stability of the LHJ switch.

### 3.3.2. LHJ switching with spermidine

Fig. 4 demonstrates that not only inorganic ions can be used to induce switching, and that the protonated polyamine spermidine, $Sp^{3+}$, appears to cause switching at relatively low concentration, consistent with its higher charge. Fig. 6a shows typical data for the titration of LHJ with $Sp^{3+}$.

It is evident that along with an increase in the ratio of the acceptor to donor HJ emission peak intensity with $c$, (as shown in Fig. 4) consistent with an increase in the proportion of closed LHJ, there is also an overall decrease in spectral intensity at all wavelengths, and as a consequence an isosbestic point is not observed. Fig. 6b also shows corresponding data for the addition of $Sp^{3+}$ to a solution of oligonucleotide **1** from the LHJ. This oligonucleotide contains only a donor fluorophore and therefore only shows donor emission, but a reduction in donor emission intensity is observed over the same concentration range as LHJ. This reduction is consistent with a decrease in donor lifetime through changes in the local donor environment, caused by $Sp^{3+}$-oligonucleotide association. This is not unexpected; $Sp^{3+}$ is abundant in living cells [30,31] and is known to play a key role in maintaining cellular DNA in a compact state. Indeed the molecular mechanism of $Sp^{3+}$ function in DNA condensation is presumed to involve neutralisation of the negatively charged phosphate groups on the DNA backbone by $Sp^{3+}$ association with DNA [32–34]; this has been supported by Raman measurements [35]. Notwithstanding the low switching concentration observed for $Sp^{3+}$, this reduction in intensity of the fluorescence output of the switch state makes protonated polyamines such as $Sp^{3+}$ less

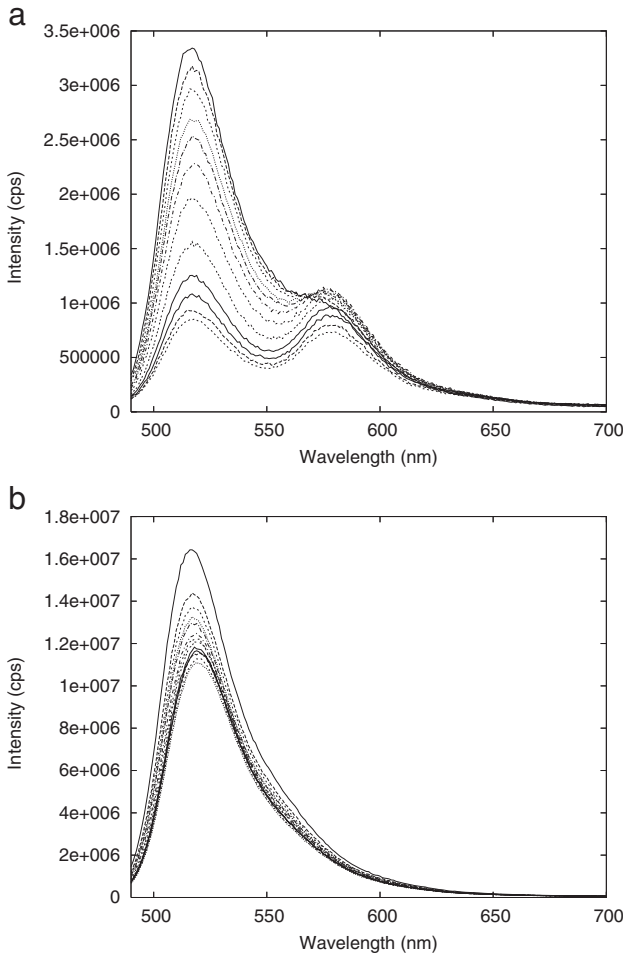


Fig. 6. Typical fluorescence emission spectra obtained when titrating (a) 1 μM LHJ and (b) 1 μM oligonucleotide 1 from LHJ only with increasing concentrations of $Sp^{3+}$ between 0 and 2.3 mM in Tris/HCl buffer.

attractive as LHJ switching ions in comparison to the inorganic ions studied.

## 4. Concluding remarks

This work shows that although both the SHJ and LHJ are a functioning switch, the SHJ is prone to dissociation in the open conformation, consistent with previous observations for other short-armed HJs. However, the LHJ does not dissociate and also retains favourable ion switching characteristics. Several inorganic ions have been shown to induce simple two-state switching, with quantitative fluorescence output of the switch state. Consistent with previous work, an increase in the valency of the switching ions has been shown to be effective in dramatically decreasing the required ion concentration for switching. However, the use of the protonated polyamine spermidine, the most widely used method for producing cations of high valency, is problematic as, although it does induce switching at low concentration, it also produces a marked decrease in fluorescence intensity on switching.

The quantitative switching characteristics obtained using inorganic ions at relatively low switching ion concentration, coupled with the potential for tailored DNA-HJ through LHJ arm sequence control, makes this system a promising candidate for use in nanoscale biomolecular devices.

## Acknowledgements

We thank R. Z. Troitzsch for supplying the schematic diagrams for Fig. 1 and H. Vass and Dr. S. W. Magennis for spectroscopy. We also thank A. M. Haughey for contribution to the practical work. This work was carried out as part of the UK Department of Trade and Industry (Beacon Project); we gratefully acknowledge this financial support and helpful discussions with our technical monitor, Marc Bailey.

## References

[1] N.C. Seeman, Biochemistry and structural DNA nanotechnology: an evolving symbiotic relationship, Biochemistry 42 (2003) 7259–7269.
[2] L. Adleman, Molecular computation of solutions to combinatorial problems, Science 266 (1994) 1021–1024.
[3] P. Sa-Ardyen, N. Jonoska, N.C. Seeman, The construction of graphs whose edges are DNA helix axes, J. Am. Chem. Soc. 126 (2004) 6648–6657.
[4] A. Carbone, N.C. Seeman, Circuits and programmable self-assembling DNA structures, Proc. Natl. Acad. Sci. 99 (2002) 12577–12582.
[5] Z. Shen, H. Yan, T. Wang, N.C. Seeman, Paranemic crossover DNA: a generalized Holliday structure with applications in nanotechnology, J. Am. Chem. Soc. 126 (2004) 1666–1674.
[6] R. Holliday, A mechanism for gene conversion in fungi, Genet. Res. 5 (1964) 282–304.
[7] D. Hargreaves, D. Rice, S. Sedilinkova, P. Artymiuk, R. Lloyd, J. Rafferty, Crystal structure of *E. coli* RuvA with bound DNA Holliday junction at 6 Å resolution, Nat. Struct. Biol. 5 (1998) 441–446.
[8] R.M. Clegg, A.I.H. Murchie, D.M.J. Lilley, The solution structure of the four-way DNA junction at low-salt conditions: a fluorescence resonance energy transfer analysis, Biophys. J. 66 (1994) 99–109.
[9] M. Ortiz-Lombardia, A. Gonzalez, R. Eritja, J. Aymami, F. Azorn, M. Coll, Crystal structure of a DNA Holliday junction, Nat. Struct. Biol. 6 (1999) 913–917.
[10] D. Duckett, A. Murchie, S. von Kitzing, D. Lilley, The structure of the Holliday junction, and its resolution, Cell 55 (1988) 79–89.
[11] S.A. McKinney, A. Declais, D.M. Lilley, T. Ha, Structural dynamics of individual Holliday junctions, Nat. Struct. Biol. 10 (2003) 93–97.
[12] D. Lilley, Structures of helical junctions in nucleic acids, Q. Rev. Biophys. 33 (2000) 109–159.
[13] D. Duckett, A. Murchie, D. Lilley, The role of metal ions in the conformation of the four-way DNA junction, EMBO J. 9 (1990) 583–590.
[14] N. Hud, J. Feigon, Localisation of divalent metal ions in the minor groove of DNA A-tracts, J. Am. Chem. Soc. 119 (1997) 5756–5757.
[15] B. Buuren, T. Hermann, S. Wijmenga, E. Westhof, Brownian-dynamics simulations of metal–ion binding to four-way junctions, Nucleic Acids Res. 30 (2002) 507–514.
[16] J.H. Thorpe, B.C. Gale, S.C.M. Teixeira, C.J. Cardin, Conformational and hydration effects of site-selective sodium, calcium and strontium ion binding to the DNA Holliday junction structure d(TCGGTACCGA)4, J. Mol. Biol. 327 (2003) 97–109.
[17] D. Lilley, All change at Holliday junction, Proc. Natl. Acad. Sci. 94 (1997) 9513–9515.
[18] B.F. Eichman, J.M. Vargason, B.H.M. Mooers, P.S. Ho, The Holliday junction in an inverted repeat DNA sequence: sequence effects on the structure of four-way junctions, Proc. Natl. Acad. Sci. 97 (2000) 3971–3976.
[19] A. Declais, J. Fogg, A. Freeman, F. Coste, J. Hadden, S. Phillips, D. Lilley, The complex between a four-way DNA junction and $T_7$ endonuclease I, EMBO J. 22 (2003) 1398–1409.
[20] P.S. Eis, D.P. Millar, Conformational distributions of a four-way DNA junction revealed by time-resolved fluorescence resonance energy transfer, Biochemistry 32 (1993) 13852–13860.
[21] A.I.H. Murchie, R.M. Clegg, E. von Kitzing, D.R. Duckett, S. Diekmann, D.M.J. Lilley, Fluorescence energy transfer shows that the four-way DNA junction is a right-handed cross of antiparallel molecules, Nature 341 (1989) 763–765.
[22] C. Joo, S.A. McKinney, D.M.J. Lilley, T. Ha, Exploring rare conformational species and ionic effects in DNA Holliday junction using single-molecule spectroscopy, J. Mol. Biol. 341 (2004) 739–751.
[23] S.M. Miick, R.S. Fee, D.P. Millar, W.J. Chazin, Crossover isomer bias is the primary sequence-dependent property of immobilized Holliday junctions, Proc. Natl. Acad. Sci. U. S. A. 94 (1997) 9080–9084.
[24] T. Shida, H. Iwasaki, H. Shinagawa, Y. Kyogoku, Characterization and comparison of synthetic immobile and mobile Holliday junctions, J. Biochem. 119 (1996) 653–658.
[25] V.R. Ramirez-Carrozzi, T.K. Kerppola, gelFRET analysis of nucleoprotein complexes, Methods 25 (2001) 31–43.
[26] B. Yurke, A.J. Turberfield, A.P. Mills Jr., F.C. Simmel, J.L. Neumann, A DNA-fuelled molecular machine made of DNA, Nature 406 (2000) 605–609.
[27] N.R. Kallenbach, R.I. Ma, N.C. Seeman, An immobile nucleic acid junction constructed from oligonucleotides, Nature 305 (1983) 829–831.
[28] S.M. Chen, F. Heffron, W. Leupin, W.J. Chazin, Two-dimensional H NMR studies of synthetic immobile Holliday junctions, Biochemistry 30 (1991) 766–771.
[29] J.N. Weiss, The Hill equation revisited: uses and misuses, FASEB J. 11 (1997) 835–841.
[30] S.S. Cohen, A Guide to Polyamines, Oxford University Press, New York, 1998.
[31] C.W. Tabor, H. Tabor, Polyamines, Annu. Rev. Biochem. 53 (1983) 749–790.
[32] L.C. Gosule, J.A. Schellman, Compact form of DNA induced by spermidine, Nature 259 (1976) 333–335.
[33] L.C. Gosule, J.A. Schellman, DNA condensation with polyamines: I. Spectroscopic studies, J. Mol. Biol. 121 (1978) 311–326.
[34] R.W. Wilson, V.A. Bloomfield, Counterion-induced condensation of deoxyribonucleic acid: a light-scattering study, Biochemistry 18 (1979) 2192–2196.
[35] H. Deng, V.A. Bloomfield, J.M. Benevides, G.J. Thomas, Structure basis of polyamine-DNA recognition: spermidine and spermine interactions with genomic B-DNAs of different GC content probed by Raman spectroscopy, Nucleic Acids Res. 28 (2000) 3379–3385.